

# Anisotropic flow of thermal photons as a quark-gluon plasma viscometer

Chun Shen\* and Ulrich Heinz

*Department of Physics, The Ohio State University, Columbus, Ohio 43210-1117, USA*

Jean-Francois Paquet, Igor Kozlov, and Charles Gale

*Department of Physics, McGill University, 3600 University Street, Montreal, Quebec, H3A 2T8, Canada*

(Dated: June 6, 2019)

We present state-of-the-art calculations of viscous photon emission from nuclear collisions at RHIC and LHC. Fluctuating initial density profiles are evolved with event-by-event viscous hydrodynamics. Momentum spectra of thermal photons radiated by these explosively expanding fireballs and their  $p_T$ -differential anisotropic flow coefficients  $v_n(p_T)$  are computed, both with and without accounting for viscous corrections to the standard thermal emission rates. Viscous corrections to the rates are found to have a larger effect on the  $v_n$  coefficients than the viscous suppression of hydrodynamic flow anisotropies. Since photons are found to be more sensitive to the quark-gluon plasma (QGP) shear viscosity than hadrons, their anisotropic flow coefficients  $v_n$  serve as a sensitive QGP viscometer.

PACS numbers: 25.75.-q, 25.75.Cj, 25.75.Ld, 24.10.Nz

The shear viscosity of quark-gluon plasma (QGP) has received much recent attention. Experimental measurements of the collective flow of the ultradense matter created in relativistic heavy ion collisions at the Relativistic Heavy Ion Collider (RHIC) and the Large Hadron Collider have shown that this matter exhibits almost perfect fluidity [1]. The observations limit the QGP shear viscosity to entropy density ratio,  $(\eta/s)_{\text{QGP}}$ , to less than  $\frac{3}{4\pi}$  [2], i.e. to less than 3 times the lowest value allowed by quantum theory [3].  $(\eta/s)_{\text{QGP}}$  is extracted from measured anisotropies in the flow pattern of the hadrons emitted from the collision fireball in its final freeze-out stage [2]. These flow anisotropies are driven by anisotropic pressure gradients in the fireball, caused by collision geometry and event-by-event fluctuations in its initial density distribution. Shear viscosity degrades the fluid's ability to convert such pressure anisotropies into flow anisotropies. It is this viscous suppression of anisotropic flow that is being exploited when extracting  $(\eta/s)_{\text{QGP}}$  from measured final state flow patterns.

All known liquids have specific shear viscosities  $\eta/s$  that depend on temperature, featuring a pronounced minimum near the liquid-gas phase transition [4]. The temperature dependence of the QGP shear viscosity is of paramount interest since a possible rise of  $(\eta/s)_{\text{QGP}}(T)$  at temperatures above the critical value  $T_c$  of the quark-hadron phase transition may indicate a gradual change of character of the QGP, from a strongly-coupled liquid near  $T_c$  to a more weakly coupled gaseous plasma at much higher temperatures. The bulk of the particles created in heavy-ion collisions are strongly interacting hadrons that escape only at the very end of the fireball's evolution and thus contain only indirect information about the hottest QGP stages near the beginning of its life. Photons, on the other hand, interact only electromagnetically and can escape from the fireball during all collision stages, especially from its hot core. Anisotropies in

the emitted photon spectra reflect flow and momentum anisotropies of the radiating QGP medium at the time of photon emission and are thus sensitive to shear viscous effects at that time. A measurement of anisotropic photon flow thus provides a window into the hot core of the QGP fireball [5], offering the chance to constrain its specific shear viscosity at high temperature  $T \gg T_c$ .

For a fixed value of  $\eta/s$ , the dynamical effects from shear viscosity are proportional to the fluid's expansion rate [1]. In heavy-ion collisions the expansion rate is highest at early times. Viscous effects on photon flow should therefore be more important than those for hadrons emitted at the end of the collision. This led Dusling [6] to propose using photons as a QGP viscometer. We expand on this idea by studying the entire spectrum of anisotropic flows generated in the event: using the standard characterization of the emitted momentum distribution in terms of azimuthal Fourier coefficients ("anisotropic flows")  $v_n$  and their associated flow angles  $\Psi_n$ ,

$$E \frac{dN}{d^3p} = \frac{dN}{2\pi dy p_T dp_T} \times \left( 1 + 2 \sum_{n=1}^{\infty} v_n(p_T) \cos[n(\phi_p - \Psi_n(p_T))] \right), \quad (1)$$

where  $\phi_p$  is the angle of the emitted particle momentum  $\mathbf{p}$  around the beam direction, we focus not just on the "elliptic flow"  $v_2$  studied in previous work [5–11], but also on the higher harmonic flow coefficients  $v_{3,4,5}$ .

Investigating higher order flow harmonics is motivated by at least two observations: First, it is known [12, 13] that shear viscosity suppresses the higher  $v_n$  coefficients more strongly than  $v_2$ . A simple scaling law proposed in [14] suggests exponential suppression with  $n^2$ , and this appears to be roughly consistent with the experimental data [15]. The slope of  $\ln(v_n/\epsilon_n)$  vs.  $n^2$  should be proportional to  $\eta/s$ . Second, measurements by the PHENIX collaboration of direct photons in 200 A GeV

Au+Au collisions established a strong excess over known pQCD sources that has been attributed to thermal radiation [16]. The measured azimuthal anisotropy of this radiation [17] implied an unexpectedly large photon elliptic flow, comparable to that of pions. Recent direct photon measurements by the ALICE collaboration in 2.76 A TeV Pb+Pb collisions at the LHC [18] confirmed these findings which challenge our current theoretical understanding of microscopic rates and/or bulk dynamics [5, 8, 9]. They prompted a novel idea to generate large photon elliptic flow through a non-perturbative pre-equilibrium mechanism involving the huge initial magnetic fields generated by the colliding nuclei [10]. By studying triangular photon flow  $v_3$ , which is purely driven by fluctuations in the initial density profile and whose direction  $\Psi_3$  is therefore randomly oriented relative to the impact parameter and magnetic field [19, 20], one can disentangle these pre-equilibrium photons from the thermal photon signal.

In an anisotropically expanding fireball, viscosity leads to anisotropic deviations of the phase-space distribution from local equilibrium that affect thermal photon emission in two distinct ways: They alter the development of hydrodynamic flow, by increasing its radial component while suppressing its anisotropies [1, 2], and they modify the electromagnetic emission rate which becomes locally anisotropic. Both the deviations from equilibrium of the constituent phase-space distributions in the locally co-moving reference frame and anisotropic medium-induced self-energies of the exchanged quanta contribute to this anisotropy. We here present a first study where all of these effects are included consistently, within approximations detailed below. Our approach involves the generalization of the rules of finite temperature quantum field theory to systems that are slightly out of thermal equilibrium, including all terms that are linear in the viscous correction  $\pi^{\mu\nu}(x)$  to the energy momentum tensor  $T^{\mu\nu}(x)$  at emission point  $x$ .

Off-equilibrium corrections to photon emission rates were studied before [6, 9, 21], but only including the viscous corrections to the distribution functions of the particles involved in the radiation process. In the QGP, where collisions are caused by the exchange of (originally massless) gluons, dynamically generated (so-called Hard Thermal Loop (HTL)) self energies must be taken into account to regulate an infrared divergence caused by very soft collisions. In a plasma with locally anisotropic momentum distributions, these HTL self energies are anisotropic, too. In previous work [21–23], the HTL-resummed quark self-energy was evaluated for spheroidally deformed momentum distributions of Romatschke-Strickland form [24]. Here we generalize the HTL resummation scheme to anisotropic distribution functions of the more general

form [25]

$$f(p) = f_0(p) + f_0(p)(1 \pm f_0(p)) \frac{\pi^{\mu\nu} \hat{p}_\mu \hat{p}_\nu}{2(e+P)} \chi(p/T), \quad (2)$$

where  $f_0(p)$  is the Bose/Fermi equilibrium distribution function,  $e$  and  $P$  are the energy density and thermal pressure,  $\chi(p/T) = (p/T)^\alpha$  with  $1 \leq \alpha \leq 2$ ,  $\hat{p}_\mu$  is the momentum unit vector, and  $\pi^{\mu\nu}$  is the shear stress tensor of the system (we ignore bulk viscosity). Below we show results for  $\alpha = 2$  where the viscous corrections grow approximately quadratically with the photon momentum. Work on adding viscous corrections to the collinear emission kernel developed by AMY [26], necessary for a complete leading-order calculation of the viscous QGP photon emission rates, is ongoing.

We ignore contributions from hard pre-equilibrium processes which tend to carry small momentum anisotropies [27]. If included they would somewhat suppress the  $v_n$  results presented here.

The rate for emitting a photon in a  $2 \rightarrow 2$  process  $1 + 2 \rightarrow 3 + \gamma$  can be written as

$$E_q \frac{dR}{d^3q} = \frac{1}{2} \int_{\mathbf{p}_1, \mathbf{p}_2, \mathbf{p}_3} |\mathcal{M}|^2 2\pi \delta^{(4)}(p_1 + p_2 - p_3 - p_4) \times f(p_1) f(p_2) (1 \pm f(p_3)), \quad (3)$$

where  $\int_{\mathbf{p}} \equiv \frac{1}{(2\pi)^3} \int \frac{d^3p}{2E_p}$ . In the QGP phase, the  $2 \rightarrow 2$  photon production channels involve quark-gluon Compton scattering and quark-antiquark annihilation whose matrix elements are well known. The logarithmic infrared divergence from soft collisions is regulated by using a HTL-resummed internal quark propagator [31, 32]. The hadronic phase is modeled as an interacting meson gas within the  $SU(3) \times SU(3)$  massive Yang-Mills approach used in many previous studies (see, e.g., Refs. [28, 29]). At tree level, this formalism contributes 8 photon-producing reaction channels involving  $\pi, K, \rho, \omega$ , and  $a_1$  mesons [30].

Viscous corrections are included to linear order in  $\pi^{\mu\nu}$ , by writing the thermal photon emission rates as

$$q \frac{dR}{d^3q}(q, T) = \Gamma_0(q, T) + \frac{\pi^{\mu\nu}}{2(e+P)} \Gamma_{\mu\nu}(q, T), \quad (4)$$

where  $\Gamma_0$  and  $\Gamma_{\mu\nu}$  represent the equilibrium contribution and the first order viscous correction to the emission rate, respectively. Since  $\pi^{\mu\nu}$  is traceless and transverse to the flow velocity  $u^\mu$ , this can be cast into

$$q \frac{dR}{d^3q} = \Gamma_0 + \frac{\pi^{\mu\nu} q_\mu q_\nu}{2(e+P)} a_{\alpha\beta} \Gamma^{\alpha\beta} \quad (5)$$

with the projection tensor [33]

$$a_{\alpha\beta} = \frac{3q_\alpha q_\beta}{2(u \cdot q)^4} + \frac{u_\alpha u_\beta}{(u \cdot q)^2} + \frac{g_{\alpha\beta}}{2(u \cdot q)^2} - \frac{3(q_\alpha u_\beta + q_\beta u_\alpha)}{2(u \cdot q)^3}. \quad (6)$$

The scalars  $\pi^{\mu\nu}q_\mu q_\nu$  and  $a_{\alpha\beta}\Gamma^{\alpha\beta}$  are most easily evaluated in the global and local fluid rest frames, respectively.

$\Gamma_0(q, T)$  and  $\Gamma^{\alpha\beta}(q, T)$  are calculated by using the decomposition (2) in Eq. (3) and collecting terms independent of and linear in  $\pi^{\alpha\beta}$ , respectively. In the hadronic phase all internal propagators in the matrix elements are massive, and we follow custom [28, 29] by ignoring medium effects on the meson masses and coupling constants.  $\pi^{\alpha\beta}$  corrections thus arise only from the explicit  $f(p)$  factors for the incoming and outgoing particles in Eq. (3). In the QGP phase, the required use of HTL-resummed internal propagators to account for dynamical quark mass generation introduces a sensitivity of the matrix elements themselves to the deviation of  $f(p)$  from local equilibrium:  $|\mathcal{M}|^2 = |\mathcal{M}_0|^2 + |\mathcal{M}_1|^2 \frac{\pi^{\mu\nu}}{2(e+P)}$ . So the emission rate receives corrections  $\sim \pi^{\mu\nu}$  from both the matrix elements and the explicit  $f(p)$  factors. For a medium described by anisotropic distribution functions of the type (2), the in-medium propagators continue to satisfy the KMS relation in the high temperature limit [33]. We can therefore simply follow [23, 34] to calculate the retarded quark self-energy with the modified distribution functions (2).

The dynamical evolution of the radiating fireball is modeled with the boost-invariant hydrodynamic code VISH2+1 [35], using parameters extracted from previous phenomenologically successful studies of hadron production in 200 A GeV Au+Au collisions at RHIC [36, 37] and in 2.76 A TeV Pb+Pb collisions at the LHC [38, 39]. We explore both Monte-Carlo Glauber (MCGlb) and Monte-Carlo KLN (MCKLN) initial conditions which we propagate with  $\eta/s = 0.08$  and  $\eta/s = 0.2$ , respectively [36–39], using the lattice-based equation of state (EoS) s95p-PCE-v0 [40]. This EoS implements chemical freeze-out at  $T_{\text{chem}} = 165$  MeV by endowing the hadrons in the hadronic phase with temperature-dependent non-equilibrium chemical potentials that keep the final stable particle ratios fixed. These chemical potentials are included in the photon emission rates from the hadronic phase. – In this work, we start the hydrodynamic evolution at  $\tau_0 = 0.6$  fm/c and end it on an isothermal hadronic freeze-out surface of temperature  $T_{\text{dec}} = 120$  MeV.

The photon spectrum is calculated by folding the thermal photon emission rates with the temperature profile from the evolving hydrodynamic medium:

$$E \frac{dN^\gamma}{d^3p} = \int \tau d\tau dx dy d\eta \left( q \frac{dR}{d^3q}(q, T) \right) \Big|_{q=p \cdot u(x); T(x)}. \quad (7)$$

This spectrum is used as weight to compute the  $p_T$ -differential anisotropic photon flow coefficients  $v_n(p_T)$  relative to the  $n^{\text{th}}$ -order charged hadron flow angle  $\Psi_n$ :  $v_n(p_T) = \langle \cos[n(\phi_p - \Psi_n)] \rangle_{p_T}$ . To reduce computing time we neglect hadronic resonance decays, exploiting the finding in [41] that the charged hadron flow angle  $\Psi_n$  agrees well with the flow angle for thermal pions.

Results for  $v_{2,3,4,5}(p_T)$  for thermal photons from central and semi-peripheral Au+Au and Pb+Pb collisions at RHIC and LHC are shown in Fig. 1. For each centrality bin and initialization model we run 1000 fluctuating events. We emphasize that such an event-by-event approach is indispensable for the higher-order flow harmonics  $n \geq 3$ . Different harmonics are plotted in different colors. The difference between solid and dashed lines illustrates the importance of including viscous corrections in the emission rates; both line styles include viscous effects on the evolution of the hydrodynamic flow in the medium.

Obviously, since the MCKLN-initialized fireballs are evolved with 2.5 times larger shear viscosity than the MCGlb fireballs, the viscous corrections to the emission rates are larger in the bottom panels of Fig. 1. After inclusion of all viscous effects (solid lines), all photon  $v_n$  are significantly smaller for MCKLN initial conditions than for MCGlb ones, in spite of the  $\sim 20\%$  larger initial ellipticity  $\varepsilon_2$  from the MCKLN model [20]. In a few cases, the event-plane  $v_4$  and  $v_5$  even become negative in the MCKLN case, driven by the large viscous corrections to the photon emission rates.

The attentive reader may notice that, before including viscous effects on the emission rates (dashed lines), the higher-order anisotropic flows generated from MCKLN initial conditions are larger than those from the MCGlb model, in spite of the larger  $\eta/s$  used in the MCKLN runs. This is because the initial temperatures are lower in hydrodynamic simulations with larger shear viscosity, in order to compensate larger viscous entropy productions. This reduces the space-time volume for photon emission from the QGP phase and increases the ratio of photons from the hadronic phase to those from the QGP phase. Since hadronic photons carry about 10 times larger flow anisotropies, the  $v_n$  of the final total photons increase.

As  $p_T \rightarrow 0$ , all photon  $v_n$  coefficients are seen to approach non-zero values. This is a feature that distinguishes (massless) photons from (massive) hadrons: it is due to the pole of the photon Bose distribution at zero momentum [42] – for hadronic bosons this pole is regulated by their rest mass. The rise and fall of all  $v_n$  with increasing  $p_T$  reflects the dominance of hadronic photon sources (which come late and thus exhibit strong flow) at low  $p_T$  and the increasing weight of QGP photons from earlier and hotter stages (where flow is weak) at higher  $p_T$  [5]. The origin of the dip around  $p_T = 0.5$  GeV in all the  $v_n$  coefficients is explained in Ref. [5]: it is due to the transition from  $\pi + \pi \rightarrow \rho + \gamma$  as the dominant radiation channel at low  $p_T$  to collision-induced  $\rho$  conversion ( $\pi + \rho \rightarrow \pi + \gamma$ ) at higher  $p_T$ . The slight shift of the dip towards higher  $p_T$  with increasing  $n$  reflects the fact that the  $v_n$  of the hadronic mesons which transfer their flow to the photons (pions at low  $p_T$ ,  $\rho$  and other heavier mesons at higher  $p_T$ ) increase  $\propto p_T^n$  at low  $p_T$ .

Comparing central (0–20%) to semiperipheral

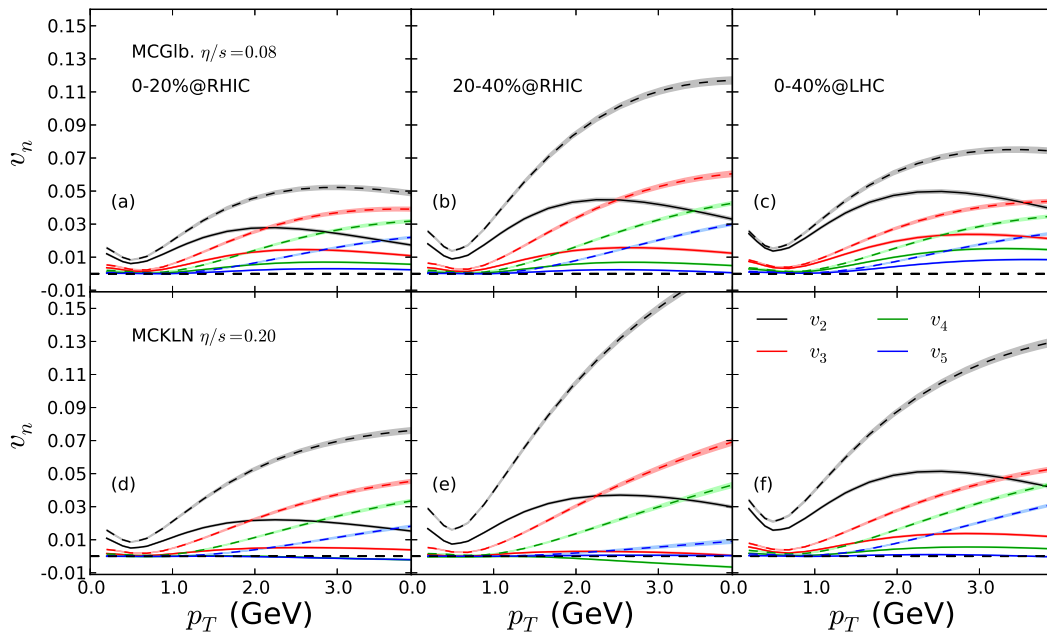


FIG. 1: (Color online) Thermal photon (QGP + Hadron Gas) anisotropic flow coefficients  $v_2-v_5$  for 200 A GeV Au+Au collisions at 0–20% and 20–40% centrality (left four panels) and for 2.76 A TeV Pb+Pb collisions at 0–40% centrality (right two panels). The upper (lower) row of panels shows results using MCGIb (MCKLN) initial conditions with  $\eta/s=0.08$  (0.2). Solid (dashed) lines depict results that include (neglect) viscous corrections to the photon emission rates. The shaded bands indicate statistical uncertainties.

(20–40%) RHIC collisions we see that only  $v_2$  increases in the more peripheral collisions, due to the increasing geometric elliptic deformation  $\varepsilon_2$  of the reaction zone. The higher-order  $v_n$  show little centrality dependence, reflecting a cancellation between increasing hydrodynamic flow anisotropies (dashed lines) and increasing shear viscous suppression of the photon emission rate anisotropies, probably due to the smaller fireball size in peripheral collisions.

Comparing RHIC with LHC collisions we find an increase of thermal photon  $v_n$  with collision energy, mainly due to the  $\sim 15\%$  longer fireball lifetime at the LHC which affects mostly the QGP phase. It allows QGP photons to develop larger flow anisotropies at LHC compared to RHIC energies. The longer fireball lifetime also helps the system to evolve closer to local thermal equilibrium. The smaller ratio  $\pi^{\mu\nu}/(e+P)$ , when averaged over the fireball history, explains the smaller difference between dashed and solid lines (reflecting the photon emission rate anisotropy) at LHC energies compared to RHIC.

The direction  $\Psi_n^\gamma$  of the  $n^{\text{th}}$ -order photon flow is obtained by computing the phase of  $\langle e^{in\phi_p} \rangle$  (where the average is taken with the  $p_T$ -integrated photon spectrum) [2]. We found that the flow angles  $\Psi_n^\gamma$  for photons from the hadronic phase are tightly correlated with the pion flow angles  $\Psi_n$ . However, the  $p_T$ -dependent viscous correction to the distribution functions in Eq. (2) leads to a decorrelation between the pion flow angle  $\Psi_n$  and the  $p_T$ -dependent photon flow angle  $\Psi_n^\gamma(p_T)$  of photons with momentum  $p_T$ . This decorrelation increases with  $p_T$  and with the shear viscosity  $\eta/s$  and is largest at early times when  $\pi^{\mu\nu}/(e+P)$  is big; it is responsible for the negative  $v_{4,5}(p_T)$  at high  $p_T$  in the two left bottom panels of

Fig. 1. It becomes weaker at LHC energies where the viscous corrections are smaller, and  $v_{4,5}(p_T)$  remain positive even for the larger  $\eta/s$  value of 0.2 (right bottom panel).

In summary, we have presented the first viscous calculation for higher order anisotropic flows of thermal photons. We find sizable triangular flow  $v_3$  for thermal photons at both RHIC and LHC energies which (by symmetry) cannot be due to the initial magnetic field. Viscous effects on the anisotropic flows of thermal photons are larger than for hadrons, due to large viscous anisotropies in the photon emission rate. This makes thermal photons ideal probes of the QGP shear viscosity at early times.

This work was supported by the U.S. Department of Energy under Grants No. DE-SC0004286 and (within the framework of the JET Collaboration) DE-SC0004104, and in part by the Natural Sciences and Engineering Research Council of Canada. The authors acknowledge useful conversations with Gabriel Denicol, Jacopo Ghiglieri, Sangyong Jeon, Yuri Kovchegov, Matthew Luzum, Guy Moore, Zhi Qiu, Ralf Rapp, Vladimir Skokov, and Gojko Vujanovic. J.-F.P. acknowledges scholarships from Hydro-Quebec and from FRQNT, and I.K. from the Canadian Institute of Nuclear Physics.

\* Correspond to shen@mps.ohio-state.edu

- [1] U. Heinz, in *Relativistic Heavy Ion Physics*, Landolt-Boernstein New Series, I/23, edited by R. Stock (Springer Verlag, New York, 2010) Chap. 5 [arXiv:0901.4355 [nucl-th]].
- [2] U. Heinz and R. Snellings, *Annu. Rev. Nucl. Part. Sci.*

- 63**, 123 (2013).
- [3] P. Kovtun, D. T. Son and A. O. Starinets, Phys. Rev. Lett. **94**, 111601 (2005).
- [4] L. P. Csernai, J. I. Kapusta and L. D. McLerran, Phys. Rev. Lett. **97**, 152303 (2006).
- [5] R. Chatterjee, E. S. Frodermann, U. Heinz and D. K. Srivastava, Phys. Rev. Lett. **96**, 202302 (2006); U. Heinz, R. Chatterjee, E. S. Frodermann, C. Gale and D. K. Srivastava, Nucl. Phys. A **783**, 379 (2007).
- [6] K. Dusling, Nucl. Phys. A **839**, 70 (2010).
- [7] R. Chatterjee and D. K. Srivastava, Phys. Rev. C **79**, 021901 (2009).
- [8] H. van Hees, C. Gale and R. Rapp, Phys. Rev. C **84**, 054906 (2011).
- [9] M. Dion, J. -F. Paquet, B. Schenke, C. Young, S. Jeon and C. Gale, Phys. Rev. C **84**, 064901 (2011).
- [10] G. Basar, D. Kharzeev and V. Skokov, Phys. Rev. Lett. **109**, 202303 (2012).
- [11] R. Chatterjee, H. Holopainen, I. Helenius, T. Renk and K. J. Eskola, arXiv:1305.6443 [hep-ph].
- [12] B. H. Alver, C. Gombeaud, M. Luzum and J. -Y. Ollitrault, Phys. Rev. C **82**, 034913 (2010).
- [13] B. Schenke, S. Jeon and C. Gale, Phys. Rev. C **85**, 024901 (2012).
- [14] P. Staig and E. Shuryak, Phys. Rev. C **84**, 034908 (2011).
- [15] R. A. Lacey *et al.*, arXiv:1305.3341 [nucl-ex].
- [16] A. Adare *et al.* [PHENIX Collaboration], Phys. Rev. Lett. **104**, 132301 (2010).
- [17] A. Adare *et al.* [PHENIX Collaboration], Phys. Rev. Lett. **109**, 122302 (2012).
- [18] D. Lohner [ALICE Collaboration], arXiv:1212.3995 [hep-ex].
- [19] G.-Y. Qin, H. Petersen, S. A. Bass and B. Muller, Phys. Rev. C **82**, 064903 (2010).
- [20] Z. Qiu and U. Heinz, Phys. Rev. C **84**, 024911 (2011).
- [21] B. Schenke and M. Strickland, Phys. Rev. D **76**, 025023 (2007).
- [22] R. Baier, M. Dirks, K. Redlich and D. Schiff, Phys. Rev. D **56**, 2548 (1997).
- [23] B. Schenke and M. Strickland, Phys. Rev. D **74**, 065004 (2006).
- [24] P. Romatschke and M. Strickland, Phys. Rev. D **68**, 036004 (2003).
- [25] K. Dusling, G. D. Moore and D. Teaney, Phys. Rev. C **81**, 034907 (2010).
- [26] P. B. Arnold, G. D. Moore and L. G. Yaffe, JHEP **0112**, 009 (2001).
- [27] S. Turbide, C. Gale, E. Frodermann and U. Heinz, Phys. Rev. C **77**, 024909 (2008).
- [28] C. Song, Phys. Rev. C **47**, 2861 (1993).
- [29] S. Turbide, R. Rapp and C. Gale, Phys. Rev. C **69**, 014903 (2004).
- [30] S. Turbide, *Electromagnetic radiation from matter under extreme conditions*, PhD thesis, McGill University (2006), UMI Thesis Server UMI-NR-25272.
- [31] J. I. Kapusta, P. Lichard and D. Seibert, Phys. Rev. D **44**, 2774 (1991) [Erratum: Phys. Rev. D **47**, 4171 (1993)].
- [32] R. Baier, H. Nakkagawa, A. Niegawa and K. Redlich, Z. Phys. C **53**, 433 (1992).
- [33] For a detailed discussion we refer the reader to a longer manuscript in preparation.
- [34] S. Mrowczynski and M. H. Thoma, Phys. Rev. D **62**, 036011 (2000).
- [35] H. Song and U. Heinz, Phys. Lett. B **658**, 279 (2008); Phys. Rev. C **77**, 064901 (2008); and Phys. Rev. C **78**, 024902 (2008).
- [36] C. Shen, U. Heinz, P. Huovinen and H. Song, Phys. Rev. C **82**, 054904 (2010).
- [37] H. Song, S. A. Bass, U. Heinz, T. Hirano and C. Shen, Phys. Rev. Lett. **106**, 192301 (2011) [Erratum: Phys. Rev. Lett. **109**, 139904 (2012)]; Phys. Rev. C **83**, 054910 (2011) [Erratum: Phys. Rev. C **86**, 059903 (2012)].
- [38] C. Shen, U. Heinz, P. Huovinen and H. Song, Phys. Rev. C **84**, 044903 (2011).
- [39] Z. Qiu, C. Shen and U. Heinz, Phys. Lett. B **707**, 151 (2012).
- [40] P. Huovinen and P. Petreczky, Nucl. Phys. A **837**, 26 (2010).
- [41] U. Heinz, Z. Qiu and C. Shen, Phys. Rev. C **87**, 034913 (2013).
- [42] U. Heinz and S. M. H. Wong, Phys. Rev. C **66**, 014907 (2002).
- [43] J.-Y. Ollitrault and F. G. Gardim, Nucl. Phys. A **904-905**, 2013, 75c (2013).
- [44] R. Chatterjee, H. Holopainen, T. Renk and K. J. Eskola, Phys. Rev. C **83**, 054908 (2011).
- [45] R. Chatterjee, H. Holopainen, T. Renk and K. J. Eskola, Phys. Rev. C **85**, 064910 (2012).
- [46] B. Schenke, S. Jeon and C. Gale, Phys. Rev. Lett. **106**, 042301 (2011).
- [47] C. Gale, S. Jeon, B. Schenke, P. Tribedy and R. Venugopalan, Phys. Rev. Lett. **110**, 012302 (2013).
- [48] Z. Qiu and U. Heinz, Phys. Lett. B **717**, 261 (2012).